

An OSCAT Simultaneous Wind/Rain GMF Appendix

Benjamin J. Fogg, David G. Long

February 2025

Abstract

The documentation for the OceanSat Scatterometer-2 (OSCAT), Tropical Rain Measuring Mission (TRMM), and European Centre for Medium-Range Weather Forecast (ECMWF) Dataset (OTED) is provided. There are 6 arrays that constitute the OTED and the contents of each are described. Tables are provided to provide further explanation of the format the 6 OTED arrays. A rudimentary analysis of the contents in the primary array *A*, and an auxiliary array *D* are presented to validate the collocation accuracy. A time series of the OTED OSCAT σ° data is provided. Some important angle definitions are discussed.

Contents

1 Overview	3
1.1 Data Sources	3
1.2 Collocation Method	3
1.3 OTED Summary	4
A The OTED Contents	4
A.1 Array <i>A</i> : Primary Data	4
A.2 Array <i>B</i> : Collocation Difference Data	6
A.3 Array <i>C</i> : Time and Location Data	7
A.4 Array <i>D</i> : OSCAT Auxiliary Data	9
A.5 Array <i>E</i> : Wind Vector Data	9
A.6 Array <i>F</i> : Retrieval Data	9
B OTE Analysis	10
B.1 Array <i>A</i> : Figures	10
B.1.1 L1B data	10
B.1.2 UHR data	12
B.1.3 L1B and UHR Comparison	14
B.1.4 TRMM Rain Rate Analysis	18
B.1.5 ECMWF Analysis	22
B.2 Array <i>D</i> Data	25

C Quality Assurance	25
C.1 OTE Time Series Analysis	25
D Angle Definitions	25
D.1 TRMM and OSCAT Incidence Angle	25
D.2 OSCAT Azimuth Angle	30
D.3 Meteorological Wind Direction	30
D.4 Relative Wind Direction	31

1 Overview

A triple collocated dataset is created from the OceanSat Scatterometer-2 (OS-CAT) normalized radar backscatter (σ°), the Tropical Rain Measuring Mission (TRMM) near-surface rain rate, and the European Centre for Medium-Range Weather Forecasts (ECMWF) near-surface vector winds (VW). The dataset is created using measurements from the 3 data sources that are temporally and spatially within 30 minutes and 1 km respectively. The dataset spans the entire mission of OSCAT available OSCAT data (2011 to 2014).

1.1 Data Sources

OSCAT operated between 2009 and 2014 [1]. It used a Ku-band rotating pencil-beam radar to measure the surface σ° . There are two beams of measurements, an inner beam and an outer beam, measured at two incidence angles, 49° and 58° . OSCAT has a polar orbit which covers the entire earth.

Three OSCAT data types are used: Level-2B (L2B), Level-1B (L1B) and Ultra High Resolution (UHR). The L1B contain the raw σ° data, while the L2B contain the VW estimates, and the UHR contain high resolution data. The L2B data are spatially sparser than the L1B making them faster to parse than the L1B data. The UHR estimates high resolution σ° values on a 2.5×2.5 km grid using the antenna response function.

TRMM operated on a Japanese satellite between 1997 and 2015 [2]. Similar to OSCAT, TRMM also operates a Ku-band radar but measures the response to rain. The incidence angle of TRMM ranges between -18 to 18 degrees. TRMM has a precipitation radar that measured the near-surface rain rates. The coverage of TRMM is restricted to near the equator.

ECMWF uses numerical weather prediction (NWP) to generate near-surface vector winds [3]. ECMWF has a product that estimates the near-surface global wind for times a day (Midnight, 6 AM, Noon, and 6 pm) on 50 km grids. The ECMWF VW are interpolated in space and time for specific locations in the collocation process.

1.2 Collocation Method

The method for collocating the datasets consists of two steps. First is an initial coarse collocation between TRMM and OSCAT L2B data locate where the the TRMM and OSCAT orbits are within 30 minutes and 1 km. Around the coarse collocations a grid of UHR σ° values are produced.

Second, a fine collocation is computed between the OSCAT (L1B, L2B, and UHR) and TRMM data. The same temporal and spatial requirements from the coarse collocations are used for the fine collocations. The ECMWF VW data is computed using trilateral interpolation for the times and locations of the finely collocated OSCAT and TRMM data.

1.3 OTED Summary

The OTED is divided into 6 arrays $A - F$. Array A contains the primary scientific data needed to create the SWR GMF. The contents of A include the OSCAT σ° for both the L1B and UHR. Along with the σ° , the A also includes the incidence angle (θ_i) of the OSCAT L1B and UHR¹. The azimuth angle (ϕ_a) is defined as being the clockwise angle between true north and the direction the antenna is pointing [4]. The ϕ_a is included (which should be distinguished from the antenna ϕ_a , which is actually included in D) for both L1B and UHR. The time and location of each specific L1B and UHR measurement is included in B .

The non-OSCAT data included in A is the TRMM surface R and PIA. The TRMM PIA measures the attenuation of the signal as it passes through the atmosphere. The ECMWF wind speed (W_s) and wind direction (\mathcal{X}_r) are calculated from the ECMWF U and V components. The time, latitude and longitude are the TRMM geographical location and times.

The five other arrays (B, C, D, E , and F) of the OTED contain supplemental information from the collocations. This data is not necessary for the SWR GMF creation but is useful for SWR GMF validation and in other atmospheric studies. The B array contains data about the temporal and spatial differences between L1B measurements and TRMM. The C array contains data about the time and location of the OSCAT measurements. The D array contains auxiliary OSCAT data like relative ϕ_a and normalized standard deviation of the communication noise of σ° measurements (K_{pc}). The E array contains supplemental VW data such as, ISRO L2B VW estimates, and U and V components from ECMWF. Finally, the F array contains the WO estimates from OSCAT σ° and theoretical WO σ° calculated from ECMWF VW.

A The OTED Contents

The OTED includes collocated σ° , VW, and R measurements from OSCAT, TRMM, and ECMWF. The data is stored in a tabular format and because there are a high number of measurements, the OTED is divided into six arrays (A, B, C, D, E , and F). Each array has the same number of rows but varies in the number of columns ($N \times M$). Where N is the number of collocations and M is the various types of data in the specific array. Each row of the arrays constitute the data for a specific collocation in the OTED.

A.1 Array A: Primary Data

The primary array, A , contains the OSCAT σ° , TRMM R and PIA, ECMWF VW, and corresponding important supplementary data needed to make the SWR GMF. Table A.1 relates the index of the column for which the OTE data is stored in A and the unit of that data.

¹The polarization of the OSCAT measurements is not explicitly included in the OTED because for OSCAT all the inner beam measurements are Horizontal polarization, while all the outer beam measurements are Vertical polarization. So, θ_i also specifies polarization.

Col	OTE Data	Unit	Col	OTE Data	Unit
1	L1B σ° IF	NS	20	UHR Inc OA	Deg
2	L1B σ° IA	NS	21	UHR Azi IF	Deg
3	L1B σ° OF	NS	22	UHR Azi IA*	Deg
4	L1B σ° OA	NS	23	UHR Azi OF*	Deg
5	L1B Inc IF	Deg	24	UHR Azi OA*	Deg
6	L1B Inc IA	Deg	25	ECMWF W_s	m/s
7	L1B Inc OF	Deg	26	ECMWF χ_r^Δ	Deg
8	L1B Inc OA	Deg	27	TRMM RR	mm/hr
9	L1B Azi IF*	Deg	28	TRMM PIA	NS
10	L1B Azi IA*	Deg	29	TRMM Inc	Deg
11	L1B Azi OF*	Deg	30	TRMM Latitude	Deg
12	L1B Azi OA*	Deg	31	TRMM Longitude	Deg
13	UHR σ° IF	NS	32	TRMM Year	-
14	UHR σ° IA	NS	33	TRMM Month	-
15	UHR σ° OF	NS	34	TRMM Day of Month	-
16	UHR σ° OA	NS	35	TRMM Hour	hr
17	UHR Inc IF	Deg	36	TRMM Minute	min
18	UHR Inc IA	Deg	37	TRMM Second	s
19	UHR Inc OF	Deg	38	TRMM Day of Year	-

Table 1: Array A - The primary OTE data with the column indices in the respective array. *The azimuth angle for OSCAT not the antenna azimuth angle but is defined as the angle between true north and the direction the antenna is pointing (see Appendix D). Δ The direction of wind is defined using meteorological wind direction (see Appendix D).

Col	OTE Data	Unit
1	L1B IF Spatial Difference	deg
2	L1B IA Spatial Difference	deg
3	L1B OF Spatial Difference	deg
4	L1B OA Spatial Difference	deg
5	L1B IF Temporal Difference	min
6	L1B IA Temporal Difference	min
7	L1B OF Temporal Difference	min
8	L1B OA Temporal Difference	min

Table 2: Array B - The columns of an auxiliary OTE array containing collocation differences in time and space between OSCAT L1B and TRMM with the column indices in the respective array.

The contents of A include the OSCAT σ° for L1B slice and UHR (the L1B footprint measurements are stored in D). Along with the σ° , the A also includes the incidence angles of the OSCAT L1B slice and UHR ². The azimuth angle is defined as being the clockwise angle between true north and the direction the antenna is pointing ³. The azimuth angle is included (not the antenna azimuth angle, which is actually included in D) for both L1B slice and UHR. The time and location of each specific L1B and UHR measurement is not included in the A .

The non-OSCAT data included in the TRMM Rain Rate (RR) and Path Integrated Attenuation (PIA). The TRMM RR is the rain near the surface of the earth [5]. The TRMM PIA measures the attenuation of the signal as it passes through the atmosphere.

The ECMWF wind speed (W_s) and direction (\mathcal{X}_r) are calculated from the ECMWF U and V components. The time, latitude and longitude are the TRMM geographical location and times. The angle of the wind direction is defined precisely defined in Appendix D.

The OSCAT measurements come in four flavors. There are 2 measurements for the inner beam and outer beam for each collocation. There is a forward and aft look for each incidence angle per collocation. The four UHR flavors are IF, IA, OF, and OA. Each individual flavor has his own incidence angle, azimuth angle, and σ° measurements. For UHR, all the measurements share the same time and location.

A.2 Array B : Collocation Difference Data

B contains the spatial and temporal differences between the TRMM and L1B slice measurements. The spatial difference is reported in terms of degrees. The conversion between degrees and km is roughly 1° to 111.11 km. The temporal

²The polarization of the OSCAT measurements is not given in the OTE because for OSCAT all the inner beam measurements are H-pol, while all the outer beam measurements are V-pol.

³See Appendix D

Col	OTE Data	Unit	Col	OTE Data	Unit
1	L1B IF Longitude	Deg	21	L1B IA Second	s
2	L1B IA Longitude	Deg	22	L1B IA Day (Y)	-
3	L1B OF Longitude	Deg	23	L1B OF Year	-
4	L1B OA Longitude	Deg	24	L1B OF Month	-
5	L1B IF Latitude	Deg	25	L1B OF Day (M)	-
6	L1B OF Latitude	Deg	26	L1B OF Hour	hr
7	L1B IF Latitude	Deg	27	L1B OF Minute	min
8	L1B OA Latitude	Deg	28	L1B OF Second	s
9	L1B IF Year	-	29	L1B OF Day (Y)	-
10	L1B IF Month	-	30	L1B OA Year	-
11	L1B IF Day (M)	-	31	L1B OA Month	-
12	L1B IF Hour	hr	32	L1B OA Day (M)	-
13	L1B IF Minute	min	33	L1B OA Hour	hr
14	L1B IF Second	s	34	L1B OA Minute	min
15	L1B IF Day (Y)	-	35	L1B OA Second	s
16	L1B IA Year	-	36	L1B OA Day (Y)	-
17	L1B IA Month	-	37	UHR Longitude	Deg
18	L1B IA Day (M)	-	38	UHR Latitude	Deg
19	L1B IA Hour	hr	39	UHR Time	Min
20	L1B IA Minute	min			

Table 3: Array C - The OSCAT temporal and spatial data (L1B and UHR) in the OTE with the column indices in the respective array.

difference is in terms of minutes. This array allows users to be more restrictive on what collocated measurements based on temporal and spatial data.

A.3 Array C : Time and Location Data

C contains the times and locations of the OSCAT L1B and UHR data. For L1B measurements the longitude and latitude and time are the same for both footprint and slice measurements. The year, month, day of month, hour, minute, second, and day of year are the temporal data that is reported and the latitude and the longitude are the spatial data that is reported. The UHR time is expressed in the number of minutes since the beginning of the year. A singular value for the time and location is reported for the four UHR σ° measurements. This is because UHR uses a reconstruction algorithm that uses multiple L1B measurements. The UHR time and location values are a composite of the locations and times of the L1B measurements that are used to calculate the UHR σ° values.

Col	OTE Data	Unit	Col	OTE Data	Unit
1	L1B IA σ^o mean	NS	17	L1B IF K_p - C	-
2	L1B IF σ^o mean	NS	18	L1B IA K_p - C	-
3	L1B OA σ^o mean	NS	19	L1B OF K_p - C	-
4	L1B OF σ^o mean	NS	20	L1B OA K_p - C	-
5	L1B IF Relative Azi	Deg	21	UHR IF K_p - A	-
6	L1B OF Relative Azi	Deg	22	UHR IA K_p - A	-
7	L1B IF Relative Azi	Deg	23	UHR OF K_p - A	-
8	L1B OA Relative Azi	Deg	24	UHR OA K_p - A	-
9	L1B IF K_p - A	-	25	UHR IF K_p - B	-
10	L1B IA K_p - A	-	26	UHR IA K_p - B	-
11	L1B OF K_p - A	-	27	UHR OF K_p - B	-
12	L1B OA K_p - A	-	28	UHR OA K_p - B	-
13	L1B IF K_p - B	-	29	UHR IF K_p - C	-
14	L1B IA K_p - B	-	30	UHR IA K_p - C	-
15	L1B OF K_p - B	-	31	UHR OF K_p - C	-
16	L1B OA K_p - B	-	32	UHR OA K_p - C	-

Table 4: Array D - The K_p constants, relative azimuth angle and mean σ^o auxiliary data with the column indices in the respective array. Generally, this data is used for wind retrieval purposes. Note Relative azimuth angle is the direction that the antenna is pointing compared to the direction the space craft is traveling.

Col	OTE Data	Unit
1	L2B Longitude	Deg
2	L2B Latitude	Deg
3	L2B Wind Direction	Deg
4	L2B Wind Speed	m/s
5	ECMWF U Component	-
6	ECMWF V Component	-

Table 5: Array *E* - Wind Vector Auxiliary data with the column indices in the respective array.

A.4 Array *D*: OSCAT Auxiliary Data

D contains complimentary data that is useful for OSCAT wind retrieval. The data included in the *D* are the L1B footprint σ° measurements, the relative azimuth angle, and the K_p constants (A, B, and C). The footprint σ° measurements reported here are actually an approximation of the footprint. They are calculated using the mean of the closest L1B slice σ° measurements where the mean σ° is calculated in normal space. The relative azimuth angle is the direction the antenna is pointing with respect to the direction the space craft is traveling. The K_p constants (A, B, and C) are used to calculate the K_p which is used in wind retrieval.

A.5 Array *E*: Wind Vector Data

E contains data that is useful for validation and debugging of the wind retrieval estimates. The L2B WV estimates along with the longitude and latitude are reported. The L2B are the ISRO conventional VW estimates. The ECMWF U and V components used to calculate the ECMWF WV.

A.6 Array *F*: Retrieval Data

The sixth array, *F*, contains the retrieval data using the OTE arrays. The L1B single measurement and mean measurement retrieved σ° is included for all four flavors of measurements. These were calculated using the ECMWF WV and the incidence and azimuth angles of the L1B data (both single measurement and mean measurement). The L1B retrieved WV is calculated using all the flavors of the L1B σ° measurements in the OTE. The UHR retrieved WV is calculated using all the flavors of the UHR σ° measurements in the OTE. The UHR retrieved WV is calculated using all the flavors of the UHR σ° measurements in the OTE.

Col	OTE Data	Unit	Col	OTE Data	Unit
1	L1B Wind Spd	m/s	10	L1B OA σ^o	NS
2	L1B Wind Dir ^Δ	Deg	11	L1B mean IF σ^o	NS
3	L1B mean Wind Spd	m/s	12	L1B mean IF σ^o	NS
4	L1B mean Wind Dir ^Δ	Deg	13	L1B mean IF σ^o	NS
5	UHR Wind Spd	m/s	14	L1B mean IF σ^o	NS
6	UHR Wind Dir ^Δ	Deg	15	UHR IF σ^o	NS
7	L1B IF σ^o	NS	16	UHR IA σ^o	NS
8	L1B IA σ^o	NS	17	UHR OF σ^o	NS
9	L1B OF σ^o	NS	18	UHR OA σ^o	NS

Table 6: Array F - The Retrieval WV and σ^o for L1B single and L1B mean and UHR with the column indices in the respective array. ^Δ The direction of wind is defined using meteorological wind direction (see Appendix D).

B OTE Analysis

The following sections are meant to understand and verify the distributions of the OTE. These figures serve as quality assurance for the data. The analysis also confirms that the collocations between TRMM and OSCAT have been performed correctly. The figures are made from the OTE that was created using option 2 spanning 2011-2014.

The figures in this section come from the data in arrays A and D . Figures generated from array B are shown in the collocation chapter. They show the collocation time and spatial disparity. No figures are generated from array C because the time and location of the TRMM data are already included in array A and the differences are already shown in the collocation chapter. Data from array E and F are mostly used for wind retrieval validation and comparison. They appear in the wind retrieval chapter.

B.1 Array A : Figures

The most important data to verify is the primary data. The primary array has the data from OSCAT, TRMM and ECMWF. This data is used to create the Rain GMF. It is important to verify that the collocations were performed correctly. This section makes sure that the distributions are correct.

B.1.1 L1B data

The σ^o distributions for L1B OSCAT data is shown in Fig. 1. The Four flavors are denoted in the title. The beams have slightly different distributions. As can be seen the inner beam has a smaller variance and a lower mean than the outer beam.

The L1B incidence angle distributions are shown in Fig. 2. Generally the incidence angles are around 49° for the inner beam and 58° for the outer beam. L1B measurements are divided into slices causing the L1B have multiple discrete

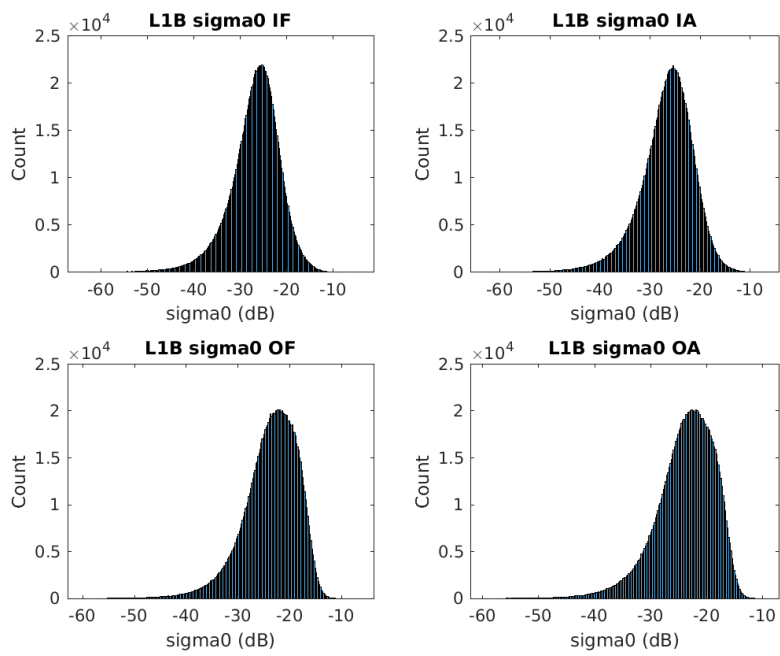


Figure 1: Distribution of L1B σ^o by look direction in dB.

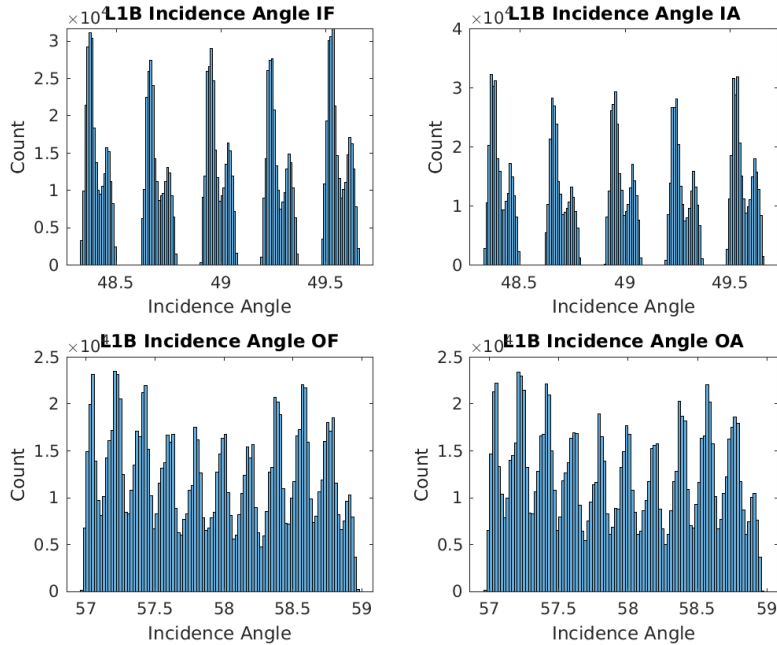


Figure 2: Distribution of L1B incidence angle by look direction in dB.

incidence angles. There are 7 slices for the inner beam and 12 slices for the outer beam. There are 5 distinct groups of incidence angles for the inner beam and there are 10 distinct incidence angle groups for the outer beam.

The azimuth angles for L1B are shown in Fig. 3. The differences between the looks is due to the fore and aft looks is due to the relative azimuth look direction. The fore looks are looking forward around 0° while the aft looks look backwards around 180° . The reason why there are distributions around 0 and 180 for both fore and aft looking measurements has to do with the definition of the relative azimuth angle compared to azimuth angle. This is explained in Appendix D. The basic difference between the two for measurements near the equator is a general offset depending on if the measurement was taken when the spacecraft was ascending or descending.

B.1.2 UHR data

The UHR algorithm takes multiple measurements from the same general location and time and uses the spatial response function and reconstruction techniques to increase the pixel resolution. The distributions of L1B and UHR is not expected to be the same but they should be similar.

The σ° distribution for UHR is shown in Fig. 4. The distributions have a high variance, since they are wide. We said that the distribution should be

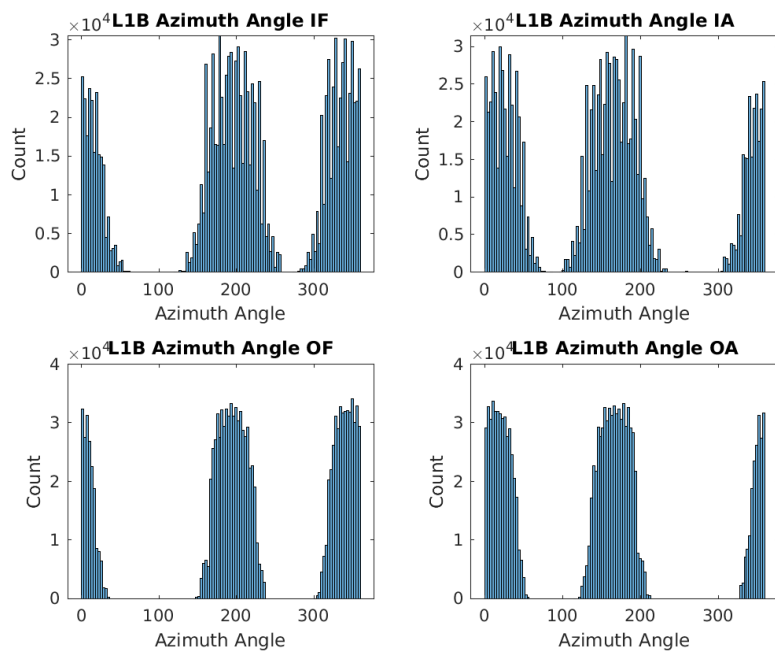


Figure 3: Distribution of L1B azimuth angle by look direction in dB.

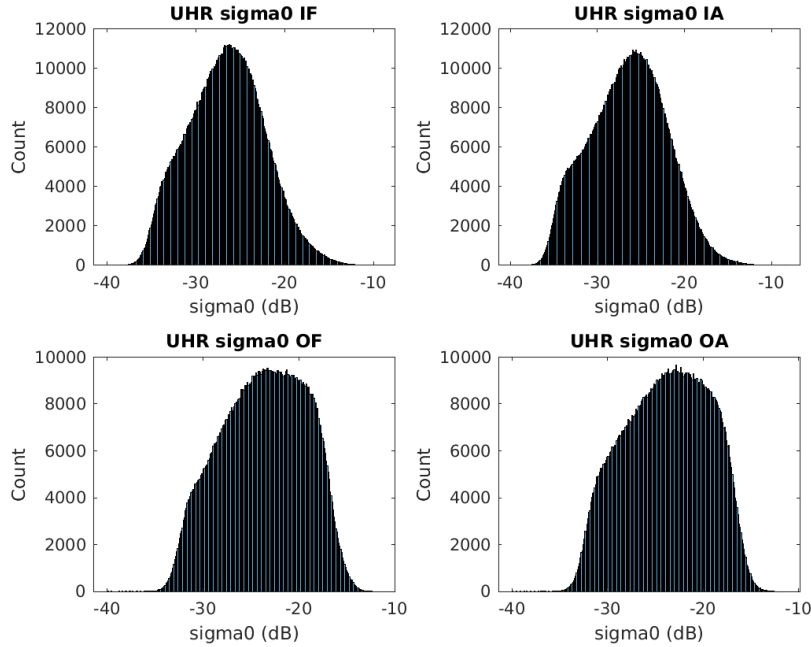


Figure 4: Distribution of UHR σ° by look direction in dB.

approximately normal, and they appear to have a bimodal distribution. The reason for the bimodal distribution is because the UHR algorithm clips the measurements at around -40 dB. This is because the UHR code was originally developed for land measurements and the σ° did not go as low as -60 dB. This phenomena can be observed when comparing the L1B to UHR directly

The incidence angle distribution is shown in Fig. 5. The distributions appear to be roughly Gaussian. This is because the incidence angles of the measurements used to calculate the σ° measurement for a pixel in the UHR array are all averaged together. By the law of large numbers, the distribution tends to be Gaussian. The azimuth angle for the UHR measurements are shown in Fig. 6. The distribution is very similar to that of the L1B. For the inner beam the azimuth angle spread is wider than that of the outer beam. The out beam azimuth angle range is smaller comparatively because the measurements in the outside edges of the outer beam swath are not used because the inner beam does not cover the same area of the outer beam.

B.1.3 L1B and UHR Comparison

It is insightful to compare the UHR and L1B distributions. The comparison helps validate the collocations are correct and understand the differences between UHR and L1B.

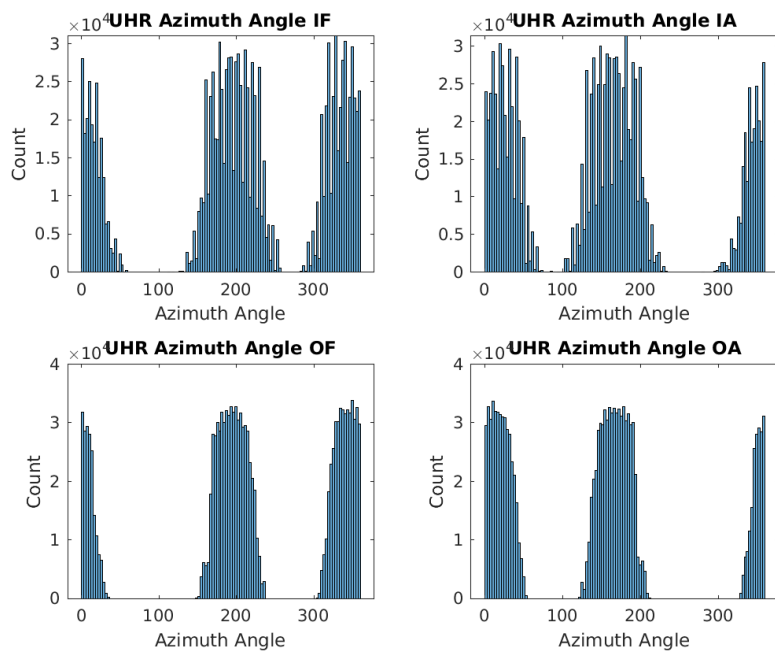


Figure 5: Distribution of UHR incidence angle by look direction.

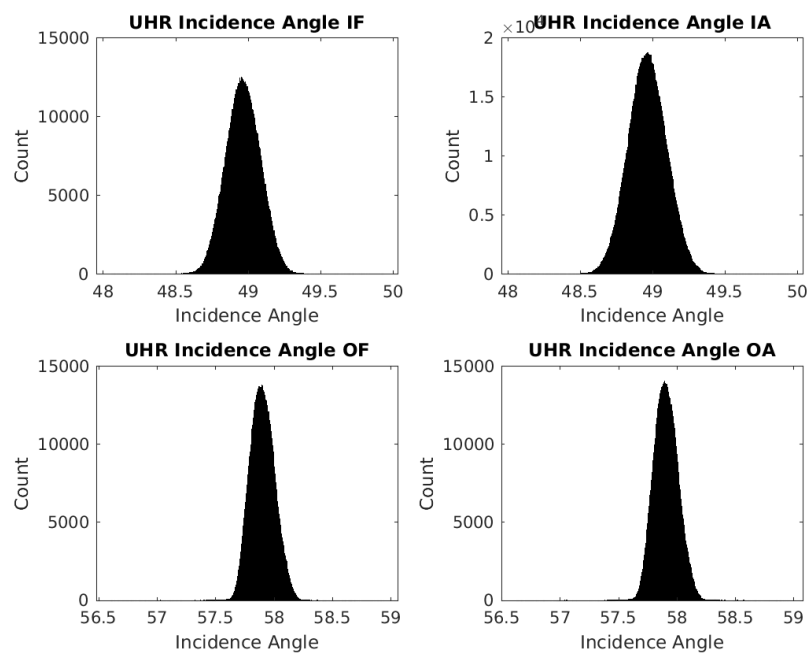


Figure 6: Distribution of UHR azimuth angle by look direction.

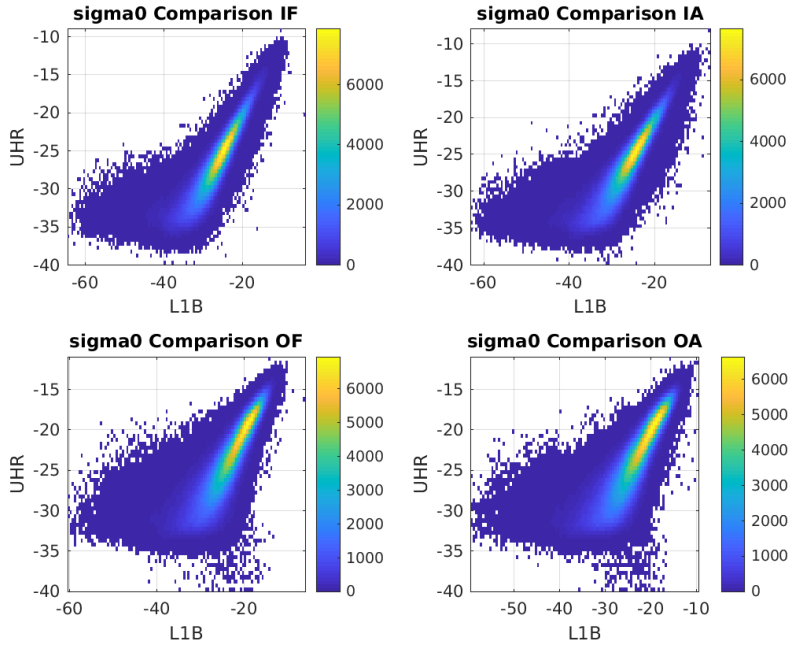


Figure 7: A two dimensional distribution comparing the L1B and UHR by look. The top left showing the inner fore look, the top right being the Inner Aft, the bottom left shows the outer fore look, and the bottom right shows the outer aft look.

The comparison between the UHR and L1B σ° are shown in Figs. 7. The figure shows that the L1B and UHR are highly correlated. Granted, there are major differences but they also appear to be related. The figure resembles a two dimensional normal distribution which is good because both L1B and UHR are supposed to be normally distributed. The L1B distribution reaches lower σ° values than UHR. UHR has a minimum of -40 dB and the L1B having a minimum of -60 dB.

The differences between the two OSCAT data types increases as the L1B σ° decreases. I believe that the differences are due to the UHR algorithm limitations in calculating small σ° values. Largest differences happen on the scale of σ° having a magnitude of 10^{-4} which is very small.

The comparison between the incidence angles of UHR and L1B are shown in Fig. 8. The angles for all the UHR and L1B measurements occur around 49° and 58° . The distributions for both resolutions are drastically different. This is due to the nature of how the incidence angle is calculated for UHR measurements. Recall that the L1B measurements are different because of the slice measurements. Each slice has a distinct incidence angle. The slices can

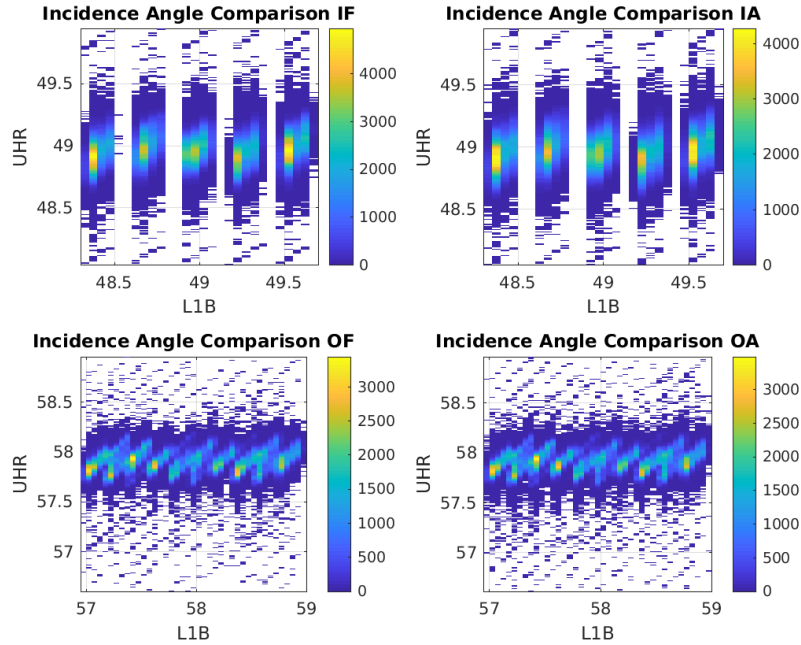


Figure 8: Histogram of the incidence angles shown in the OTE. The top shows the L1B distribution and the lower shows the distribution of the UHR.

be seen as the diagonal lines in light blue. the UHR measurements average all incidence angles used to calculate the different pixels. This includes a wide range of incidence angles from each slice which results in a normal distribution of incidence angles. Even though the distributions are drastically different, both distributions are around the correct values. These results verify that the collocations are correct.

A comparison of the UHR and L1B azimuth angle distributions is shown in Fig. 9. The azimuth angle when plotted make a line through the origin and with a slope of 1. The differences between the two distributions is minimal. There are a couple measurements that have a 360° difference. This difference is essentially 0 when dealing with degrees. The minimal differences between the two distributions show that the collocations are lined up correctly.

B.1.4 TRMM Rain Rate Analysis

The Tropical Rain Measuring Mission (TRMM) employs a precipitation radar to measure the attenuation of the signal through the atmosphere. From the attenuation of the signal, the rain rate in the area can be calculated. These datasets are very important for calculating the raing GMF.

The first TRMM data type included in the OTE is the near surface rain.

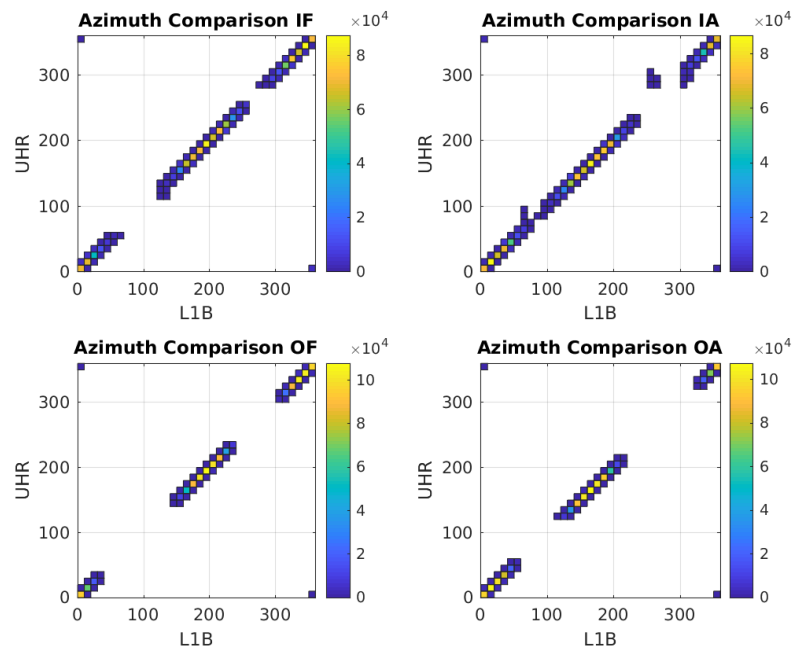


Figure 9: Histogram of the incidence angles shown in the OTE. The top shows the L1B distribution and the lower shows the distribution of the UHR.

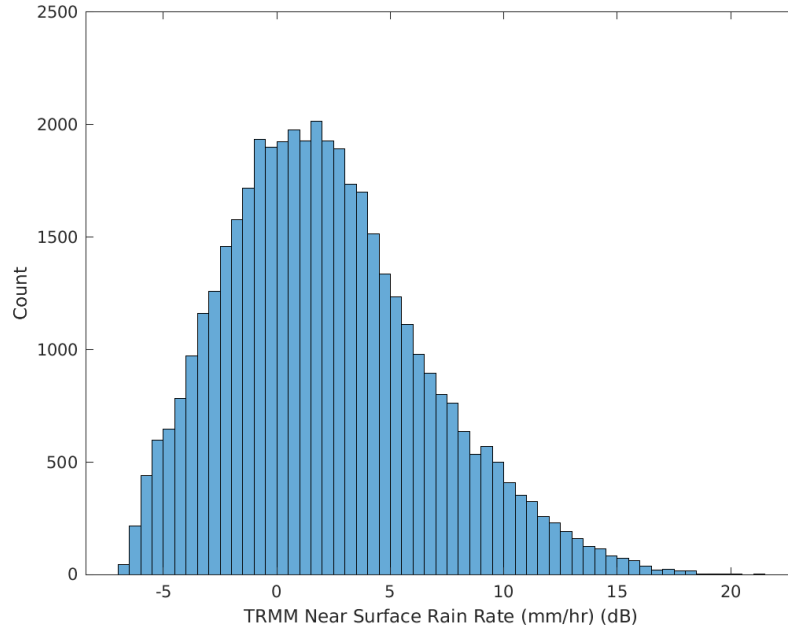


Figure 10: The distribution of rain rate

A distribution of the rain distribution can be seen in Fig. 10. The rain rate is shown in dB. The rain rate extends up to 20 dB, which is 100 mm/hr. The distributions discards all measurements that are equal to zero.

The second TRMM dataset is the PIA. The PIA distribution in the OTE is shown in Fig. 11 in dB. Something to note is that the distribution for PIA is very similar to the rain rate. The rain rate is calculated from the PIA, so the fact that they are so similar is welcomed news.

An analysis of rainy measurements by wind speed is insightful for the creation of the OTE. The wind speed bins are 0.1 m/s. In the figure it can be seen that some of the wind speeds are noisier than other wind speed bins. From 2.5 m/s to 12 m/s the noise is very low. This is because there are a lot of measurements in the wind speed bins. The higher wind bins are much nosier because of the lack of measurements. It can be seen that the percentage of rainy measurements in each wind speed bin increases as the wind speed increases. This is due to the fact that rain generally occurs when there is a storm which is accompanied by high wind (e.g., hurricanes).

Comparing the distributions of the wind speed and rain confirms that the two are uncorrelated. Fig. 12 shows the two dimensional distribution of the log count of measurements in each wind speed and rain rate bin. This result is somewhat puzzling due to the fact that storms generally result in higher

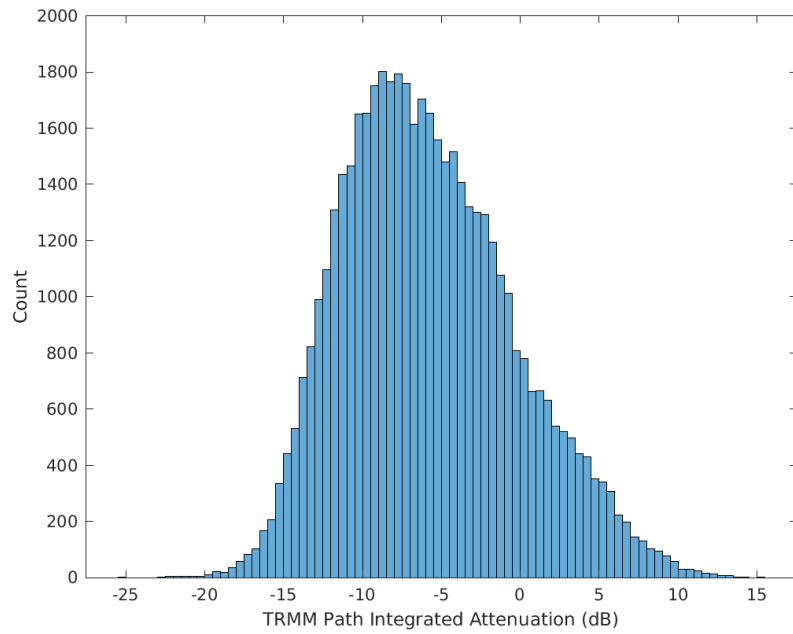


Figure 11: The total number of collocations per year is shown in blue. the rainy measurements per year are shown in red.

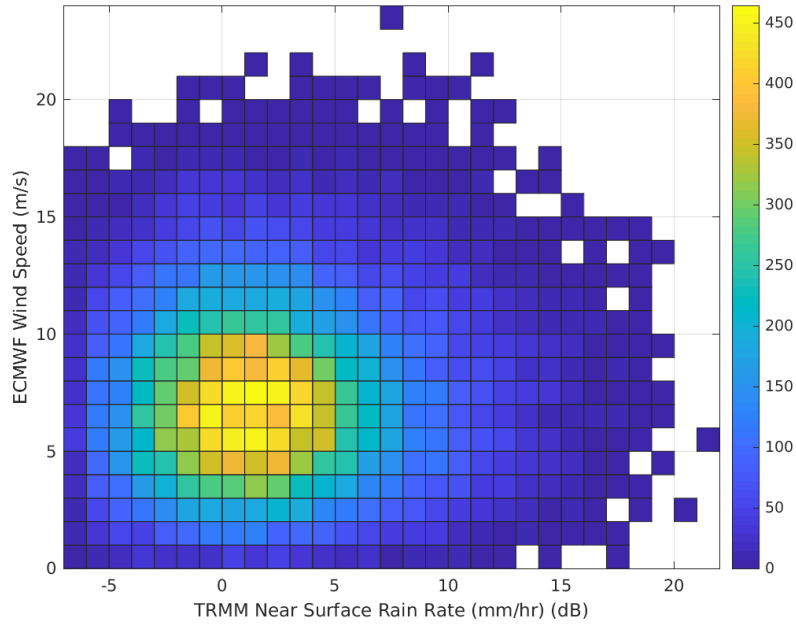


Figure 12: A histogram of the PIA in dB.

winds and rain but none the less the results are controlled by the atmospheric attributes.

The final analysis using the TRMM data is the number of rainy collocations there are per year. This is shown in Fig. 13. This figure is insightful in showing how few measurements are rainy compared to the number of collocations. It can be seen that there are less collocations during 2011 and 2014 compared to 2012 and 2013.

B.1.5 ECMWF Analysis

The ECMWF winds are important to analyze to ensure that the calculations from the ECMWF U and V components are correct. the wind speed and direction are calculated from the u and v components. Fig. 14 shows the two dimensional histogram of number of measurements of the ECMWF winds in each wind speed and direction bin. The figure shows that there is a directional bias at about 270° . Generally speaking wind speeds are on average 7 m/s. This can be seen clearly in the figure. This emphasizes the point made above in that the wind direction is essentially uniformly distributed while the wind speed is most common at 7 m/s.

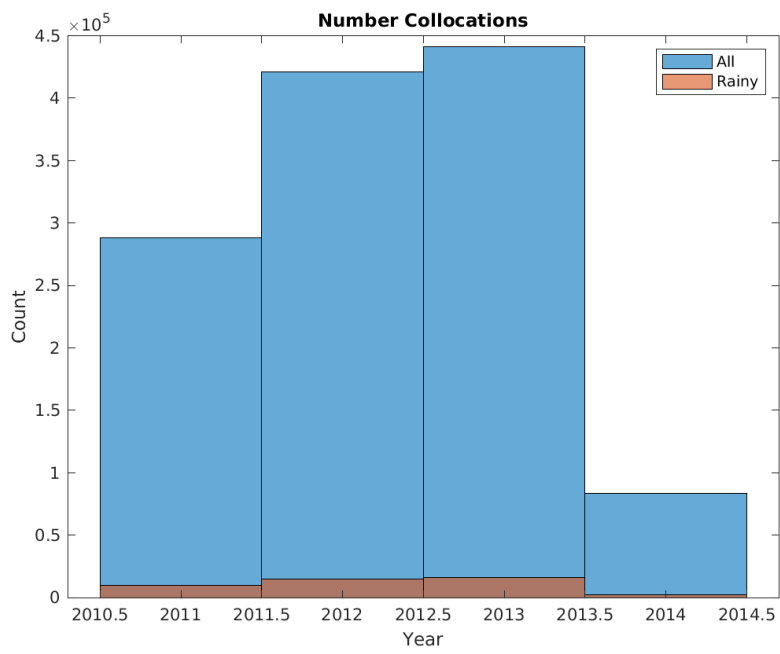


Figure 13: The total number of collocations per year, and rainy measurements in each year.

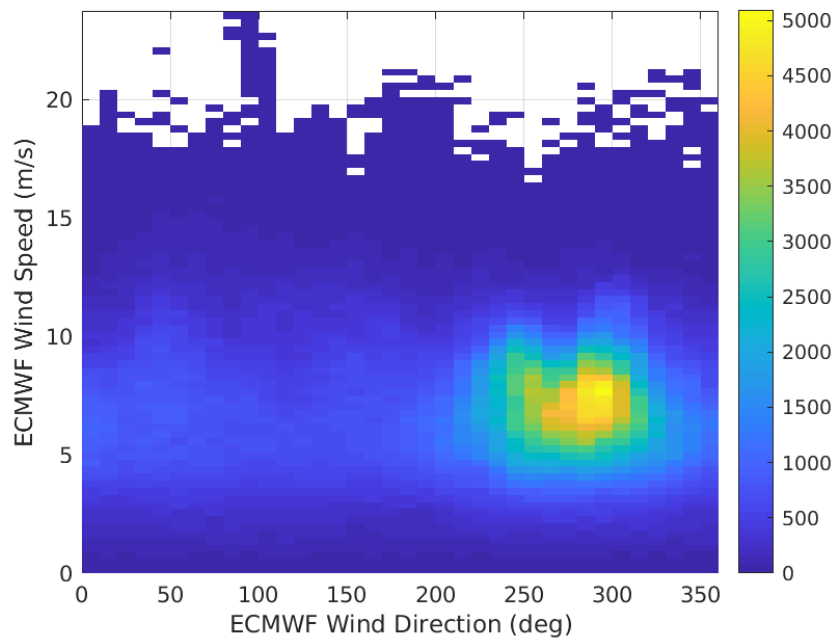


Figure 14: Two dimensional histogram showing the number of measurements in each wind speed and direction bin.

B.2 Array D Data

Array D is populated with data necessary for wind retrieval. The four data types contained in the array are the relative azimuth angle from L1B data, and K_{pc} α , β , and γ coefficients from UHR and L1B. The distribution of relative azimuth angle and the K_p coefficients are not included here because they are not essential for the narrative of this project.

The relative azimuth angle distribution is remarkably similar to the azimuth angle distributions. The important difference is there is only a single distribution for the fore and aft distributions. The reason for the azimuth angle having 2 distributions is because of the constant offset depending on whether the measurement is from an ascending pass or descending pass.

The comparing the K_{pc} distributions between UHR and L1B further validates the collocations in the OTE. A similar result happens for the K_{pc} distributions that occur for the incidence angle resolution comparison. The UHR constants are approximately normally distributed while the L1B constants distributions have artifacts from the different slices of OSCAT measurements.

C Quality Assurance

C.1 OTE Time Series Analysis

OSCAT was launched in 2009 and began operation in 2011. From 2011 to 2014 OSCAT operated with few interruptions. In 2014 the OceanSat Scatterometer stopped functioning. The death of OSCAT is visible in the OTE dataset. Analysis of the 2014 OTE data shows that there is an explainable bimodal distribution for the σ° data. Generally, the σ° should resemble Fig. 1 that have a normal distribution.

To investigate the anomaly of the σ° data in 2014 a time series of the mean of the σ° data per day using the OTE is created. This time series is shown in Fig. 15. Each dot is the mean for each day in the OTE of a specific look flavor. The years are denoted by the dashed lines. In 2014, there is a distinct step function with the mean of the OSCAT data.

The step function can be explained by the fact that OSCAT died in 2014. The data after the 54th day of 2014 is poor quality. This is shown in Fig. 16. There is a distinct difference between the data before and after the step function. The data after the step function is not included in the OTE.

D Angle Definitions

D.1 TRMM and OSCAT Incidence Angle

In making the rain GMF for OSCAT, the incidence angle (θ_i) of a OSCAT is very important in Path Integrated Attenuation (PIA) correction. OSCAT L1B data [1] does not include a PIA estimate. Attenuation of the transmitted

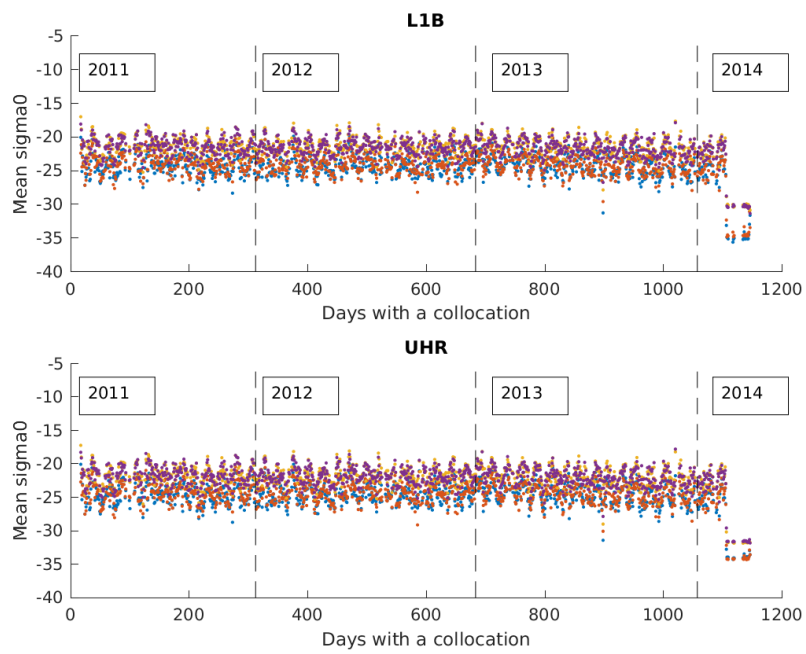


Figure 15: A time series of the σ° data from the OTE. The mean of each day is plotted for each look flavor. The dashed lines denote each year in the OTE.

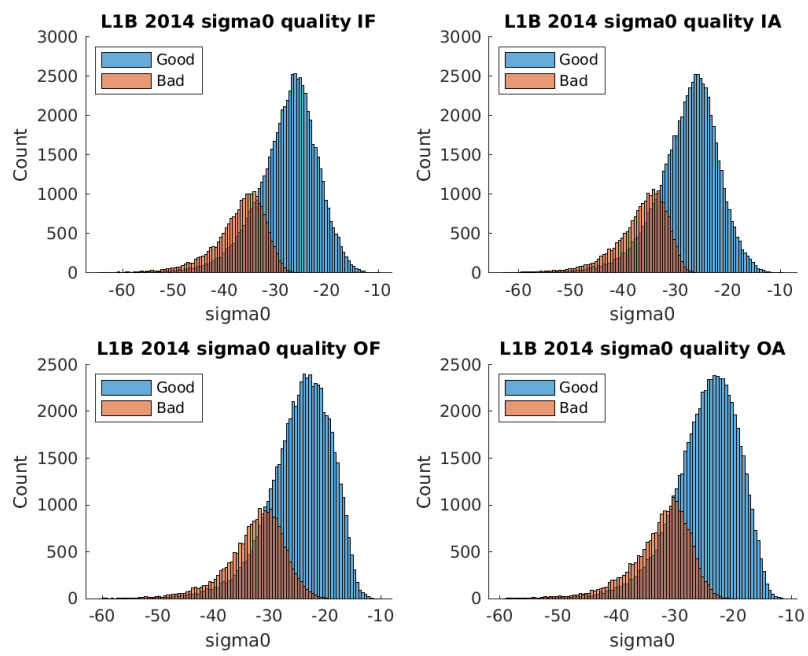


Figure 16: Two distributions shown for each look flavor of 2014. The distribution in blue is of data before the OSCAT breakdown. The distribution in red is the data after the OSCAT breakdown.

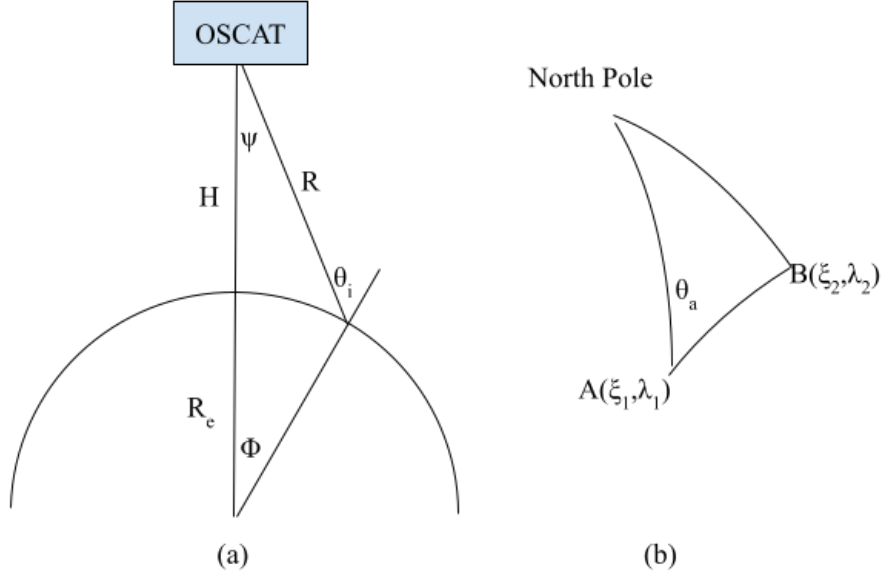


Figure 17: Graphical representation of OSCAT (a) incidence angle and (b) azimuth angle.

signal is critical to the creation of the rain GMF. The method PIA method used the TRMM attenuation as an estimate for the OSCAT PIA. θ_i of OSCAT and TRMM are used to convert PIA from TRMM geometry to OSCAT geometry.

The OSCAT θ_i is used to convert PIA from TRMM geometry to OSCAT geometry. The OSCAT definition of the incidence angle is shown graphically in Fig. 17. θ_i is defined as the angle between the normal vector at the measurement and the slant angle,

$$\frac{\sin(\psi)}{R_e} = \frac{\sin(\phi)}{R} = \frac{\sin(\theta_i)}{H}, \quad (1)$$

where R_e is the radius of the earth, R is the slant range of OSCAT, and H is the orbit height of OSCAT. The next equation enables to solving for the incidence angle,

$$R^2 = H^2 + R_e^2 - 2HR_e \cos(\phi). \quad (2)$$

TRMM reports a scan angle. The scan angle is defined as being the angle between the vector pointing straight down and the look direction. This is defined in [2] and can be seen in Fig. 18. The OSCAT incidence angle and TRMM scan angle are not consistent in their definitions.

To calculate the PIA for OSCAT, a geometric conversion needs to take place between two angles that are consistent. OSCAT documentation defines the scan angle to be 42.66° for the inner beam and 49.22° for the outer beam [1]. The PIA can be converted using the scan angles.

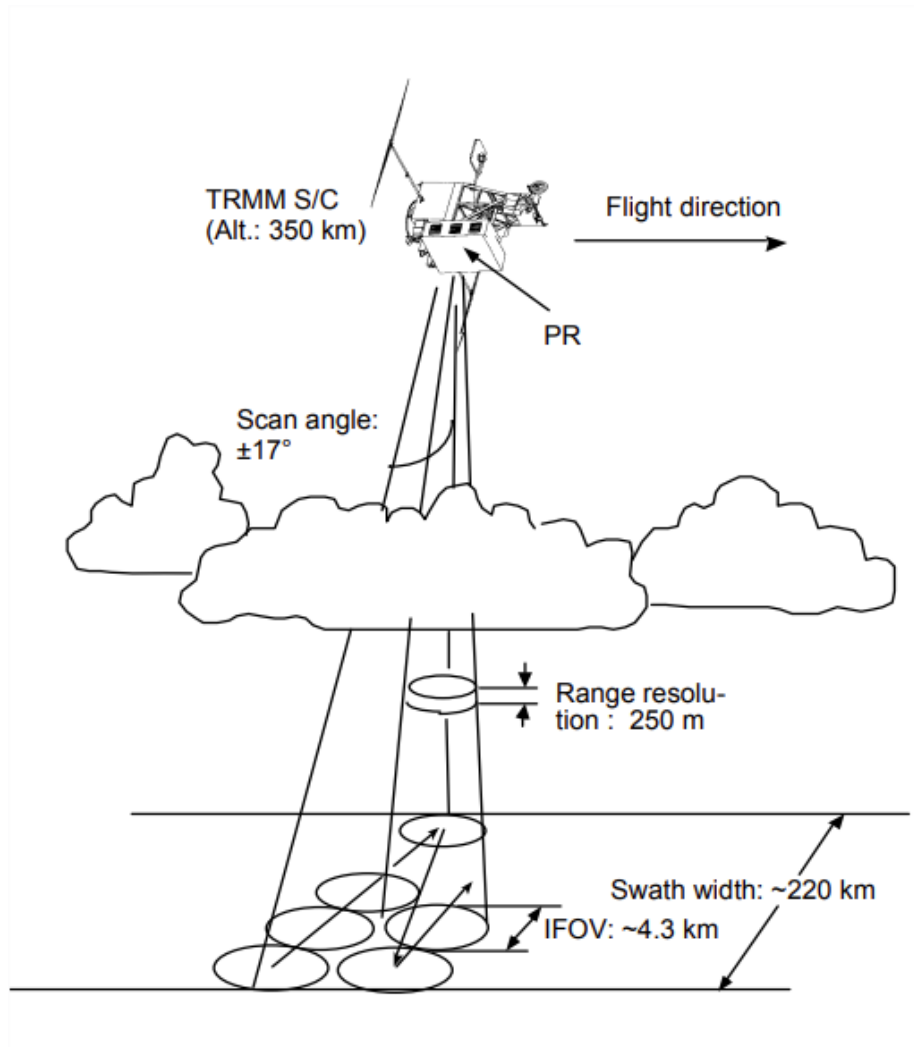


Figure 18: The scan angle of TRMM can be seen as the angle between straight down and the look angle. Taken from [2].

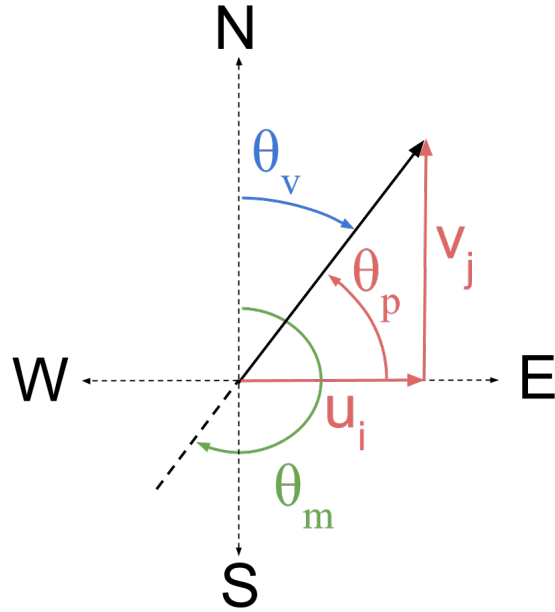


Figure 19: The wind direction, using meteorological and vector methods, and the wind components.

D.2 OSCAT Azimuth Angle

The azimuth angle (θ_a) is extremely important for estimating the wind direction from OSCAT measurements. θ_a is used to relate relative wind direction from the wind estimates to absolute wind direction. θ_a can be defined in different ways depending on the satellite. For OSCAT, θ_a is defined as the angle from from north to the angle the direction that the antenna is pointing as seen in Fig. 17. θ_a is calculable using,

$$\tan(\theta_a) = \frac{\cos(\xi_2) \sin(\lambda_2 - \lambda_1)}{\cos(\xi_1) \sin(\xi_2) - \sin(\xi_1) \cos(\xi_2) \cos(\lambda_2 - \lambda_1)}, \quad (3)$$

where (ξ_1, λ_1) and (ξ_2, λ_2) constitute a line in the direction the antenna is pointing.

D.3 Meteorological Wind Direction

The direction and speed of the wind is important for estimating wind speed and direction for OSCAT. There are two different conventions for wind direction: the oceanographic convention and the meteorological convention. The difference between the two directions is 180 °. The wind vector points in the way the wind is blowing where the meteorological direction points in the direction the wind came from.

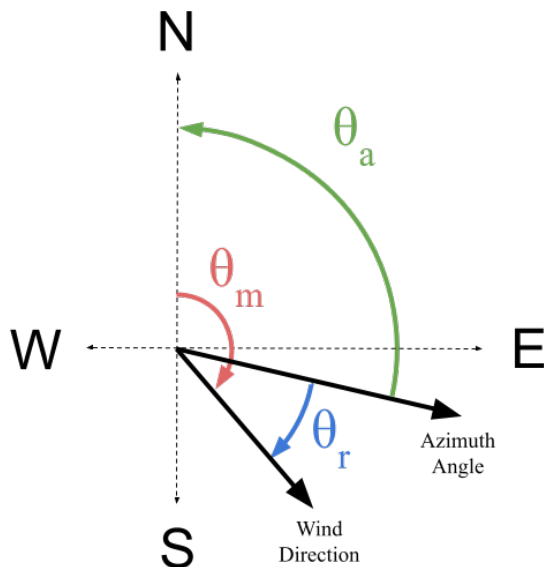


Figure 20: Graphical representation of the relative wind direction.

The definition of the meteorological wind direction is the angle between north and vector from which in the wind is blowing in the counter clockwise direction (Fig. 19). Using the methods shown in [4], the meteorological wind direction can be calculated using,

$$\theta = \tan\left(\frac{u_i}{v_j}\right) - 180, \quad (4)$$

where u_i is the zonal velocity, the component of the wind blowing towards the east, and v_j is the meridional velocity, the component of the wind blowing towards north. For this project ECMWF reports the wind speed and direction through the u_i and v_i components. The meteorological wind direction is calculated using the method above.

D.4 Relative Wind Direction

To do wind retrieval using the scatterometer data, it is important to be able to switch between relative and absolute wind direction. Using the geophysical model function, the possible wind vector solutions are given in relative wind direction. We can use the following equations to calculate the absolute wind direction from the azimuth angle and the relative wind direction,

$$\theta_r = \theta_m - \theta_a, \quad (5)$$

where θ_r is the relative wind direction, θ_m is the meteorological wind direction, and θ_a is the azimuth angle. This is depicted in Fig. 20.

References

- [1] SCAT-DP TEAM, “Oceansat-2 Scatterometer algorithms for sigma-0, processing and products format,” user manual, Advanced Image Processing Group, Signal and Image Processing Area, Space Applications Centre, Gujarat, India, 4 2010.
- [2] Precipitation Radar Team, “Tropical Rainfall Measuring Mission (TRMM) Precipitation Radar Algorithm,” user manual, TRMM Precipitation Radar Team (JAXA and NASA), USA, 7 2011.
- [3] A. Persson and F. Grazzini, “User guide to ECMWF forecast products,” *Meteorological Bulletin*, vol. 3, no. 2, 2007.
- [4] National Oceanic and Atmospheric Administration (NOAA), “WindSat Data Processing Documentation,” Technical Report WindsatDocJan06-1, National Oceanic and Atmospheric Administration (NOAA), 2006. Accessed on 2024-05-07.
- [5] D. Roddy, J. Linwood, and D. G. Long, *Satellite communications*. McGraw-Hill, New York, 5 ed., 2024.